Osmotic pressure and transport coefficient in ultrafiltration: A Monte Carlo study using quantum surface charges

Francesco Petrosino, Yannick Hallez, Giorgio de Luca, Stefano Curcio

Osmotic pressure and transport coefficient in ultrafiltration: A Monte Carlo study using quantum surface charges

F. Petrosino [a], Y. Hallez [b], G. De Luca [c], S. Curcio [a]

[a] Department of Computer Engineering, Modeling, Electronics and Systems (D.I.M.E.S.), Laboratory of Transport Phenomena and Biotechnology, University of Calabria, Ponte P. Bucci, cubo 39/c, 87036 Rende, CS, Italy
[b] Laboratoire de Génie Chimique, Université de Toulouse, CNRS, INPT, UPS, Toulouse, France
[c] Institute on Membrane Technology, ITM-CNR, Ponte P. Bucci, cubo 17/c, 87036 Rende, CS, Italy

GRAPHICAL ABSTRACT

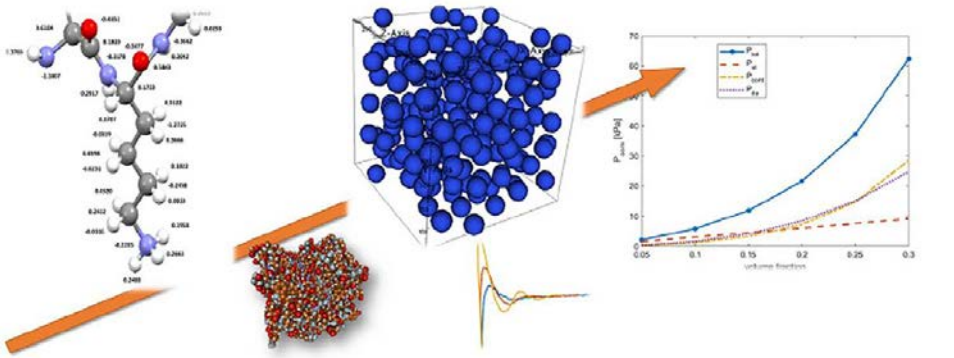

ABSTRACT

The calculation of the Osmotic Pressure and the Diffusion Coefficient, characterizing the cake layer developing during the Ultrafiltration (UF) of Bovine Serum Albumin (BSA), through a Multiscale Model based on Quantum Mechanics (QM) and Monte Carlo methods (MC) was the aim of this work. From the *ab initio* results described in previous works, the distribution of the BSA surface charges was used. A home made Metropolis MC algorithm, aimed at simulating the formation of BSA loose or concentrated layers during membrane operations, was also implemented. In such a MC algorithm, a DLVO energy calculation methodology of the adsorbed system was developed. Different MC simulations and Hypernetted Chain theory (HNC) calculations were performed so to determine both the Osmotic Pressure and the Diffusion Coefficient of BSA according to the Chun and Bowen approach, thus allowing a comparison between the calculated values of osmotic pressure and a set of experimental data taken from the literature. Such a comparison showed a good agreement between the simulated and the experimental results.

Keywords:
Multiscale modeling
Ab-initio modeling
Theory of liquids
Computational chemistry
Membrane fouling
Bovine serum albumin

1. Introduction

On an industrial scale, membrane processes have been proved to be effective and economically attractive in a variety of processes, e.g. protein recovery, pharmaceutical or oil water separations, alcohol or latex recovery (Cheng et al., 1998; Chakraborty et al., 2017). The separation and purification of bio products such as proteins, protein hydrolysates, polysaccharides, vitamins and amino acids are important steps in the food industry due to the large number of possible applications (Zin et al., 2016; Nath et al., 2014). In particular, UltraFiltration (UF) is widely used in colloidal dispersions treatment and has become a standard method in protein recovery due to its good performance in terms of cost and selectivity (Saha et al., 2017).

However, UF has a number of downsides, the major one being the flux reduction during permeation. Such a problem is due both to concentration polarization (CP), a reversible phenomenon referred to the development of concentration gradients at a membrane/solution interface, and to membrane fouling, an irreversible phenomenon, which is due either to solute deposition on the membrane surface forming a gel layer or to solute adsorption inside the pore structure and over the membrane (Suki et al., 1984).

The interplay between osmotic pressure and applied transmembrane pressure (TMP) is responsible for CP and fouling formation and strongly affects membrane performance. Four classes of models have been proposed in the literature to describe membrane fouling; each of these models takes into account the actual characteristics of both the membrane and the solute(s) dispersed in the solution to be filtered (Bolton et al., 2006).

In particular, with reference to the cake filtration model, in order to properly predict the behavior of UF process, it is necessary to precisely calculate both the additional resistance, R_{add}, to permeate flow and the osmotic pressure $\Delta\pi$, related to the solute concentration, which, evaluated at the membrane surface, leads to a decrease in the driving pressure that is equal to $\Delta\pi$.

Many models aimed either at the description of the fouling formation during UF through stochastic approaches or at the calculation of osmotic pressure were formulated. *Chen Y. and Kim H.* proposed an on lattice Monte Carlo model referred to a two dimensional membrane pore and surface and simulated the pore blocking and the cake formation (Chen and Kim, 2008). *J. Flora* proposed a stochastic approach to model the fouling of ultrafiltration membrane surfaces (Flora, 1993). *Bowen W. et al.* proposed a mathematical *a priori* model for predicting osmotic pressure of electrostatically stabilized colloids in UF process; the colloidal interactions were described by the Wigner Seitz cell approach and the osmotic pressure calculation was essentially based on the addition of different contributions to the interaction energy in agreement with the extended Deryaguin Landau Verwey Overbeek (DLVO) theory (Bowen and Williams, 1996). *Roa R. et al.* proposed different approaches to calculate the Osmotic Pressure of solutes accumulating on the membrane surface during the UF process; in particular, either a macroscopic description of cross flow UF of non ionic microgels modeled as solvent permeable spheres (Roa et al., 2015) or a theoretical description based on the one component macroion fluid model (OCM) (Roa et al., 2016) were proposed.

However, these papers and many others available in the literature, do not contain a complete multi scale approach, actually oriented to the simulation of UF process starting from the ab initio knowledge acquired at sub nanoscopic scale. In most of the papers, only partial multi scale pathways, which generally describe the system behavior at a mesoscopic scale or are based on a set of experimental parameters such as the colloidal charge, have been developed.

The actual aim of a complete multi scale approach is to provide a comprehensive, theoretical model, which can predict macromolecules structuration or aggregation and, then, the permeate flux decay typical of UF, starting from fundamental quantities, namely the electrostatic surface charges of the macromolecule under study, resulting from the *ab initio* calculations.

Two papers describing a complete multi scale model for the simulation of UF processes were already published by some of the authors of the present work (De Luca et al., 2014; Curcio et al., 2018). The first one (De Luca et al., 2014) had to be considered as a "first brick" for the formulation of a more comprehensive and accurate modeling approach aimed at predicting the behavior of protein purification by UF. In fact, the noncovalent interactions existing between the protein molecules and the membrane surface, which significantly affect membrane permeability during UF (Szymczyk and Fievet, 2005), were not taken into account. In the second paper (Curcio et al., 2018), the noncovalent proteins surface interactions were accurately evaluated by a quantum and molecular mechanics approach. This *ab initio* modeling allowed defining the actual structure of the first layer of adsorbed proteins and the equilibrium distance among them. In this way, a physical limit to both the volume fraction and the additional resistance, as due to adsorbed macromolecules, was rigorously calculated. However, in these papers (De Luca et al., 2014; Curcio et al., 2018; Petrosino et al., 2019) only the interactions between a limited number of macromolecules and the surface was analyzed. Nevertheless, the methods used to simulate the phenomena in mesoscopic and macroscopic scales were founded on a major assumption: the formation of the protein deposit layers towards the bulk, in fact, was simulated through a force balance written with reference to a specific protein packing symmetry that yielded a compactly ordered cake. Although, the noncovalent proteins surface interactions were accurately evaluated by a quantum and molecular mechanics approach (De Luca et al., 2014; Curcio et al., 2018) and, as a result, the structure of the first layer of proteins adsorbed on membrane surface was obtained by calculating the equilibrium distance between them, a body centered cubic structure symmetry was assumed. A physical limit for both the volume fraction and the additional resistance, as due to either the compact or the loose proteins deposit, was rigorously calculated presuming that this symmetry held also for the loose layers.

The present paper, starting from the fundamental parameters already calculated in the described articles, is intended to propose a stochastic procedure for the simulation of cake layer formation during UF processes without exploiting any protein packing assumptions. In addition, the calculations of the osmotic pressure and of the diffusion coefficient of BSA in the cake have been performed more rigorously, using this calculated structure.

A Metropolis Monte Carlo procedure has been implemented in a home made algorithm. A number of simulation boxes large enough to be representative of the proteins layers were analyzed. The potential energy calculation relied on the DLVO pair potential, with a Yukawa model for electrostatic interactions and a van der Waals contribution. Periodic boundary conditions were enforced in the 3 space directions to simulate a large enough volume as compared to the colloid scale but small enough as compared to a macroscopic concentration polarization layer.

It was therefore possible to calculate the osmotic pressure of the deposit layer as a function of the volume fraction related to the total potential characterizing the considered box system. From the generalized virial pressure equation, the formulation for the osmotic pressure calculation was obtained (Roa et al., 2016; Deserno and von Grünberg, 2002; Hansen and McDonald, 2006). Moreover, the diffusion coefficient was evaluated by the approaches based on the *Donnan* equilibrium (Stell and Joslin, 1986) and *Kirkwood and Buff* theory (Braga et al., 2018) as exploited in *Roa R. et al.* papers (Roa et al., 2016; Roa et al., 2015).

It is worthwhile remarking that the present model did not make use of any adjustable parameter since its inputs were represented by fundamental quantities calculated by ab initio methods; this allows developing a computational tool capable of accurately simulating colloids adsorption in UF process without resorting to any empirical or adjustable parameter.

2. Theoretical

2.1. Quantum mechanics calculations

The protein surface charges are necessary to evaluate the electrostatic short and long range interactions by the present multi scale approach. The distribution of surface charges depends on

the arrangement and of the nature of external amino acids, as well as on the experimental conditions such as type of solvent, pH, sol vated ions, etc. The considered crystallographic structure of BSA, as reported in the pbd file, is referred to a stable structure at pH val ues ranging from 4.5 to 8 (Barbosa et al., 2010) taking into account the BSA adaptable nature. Thus, the external amino acids defining the protein surface were preliminarily identified. A home made algorithm was implemented so as to obtain the coordinates of the BSA external amino acids from its crystallographic structure. (Curcio et al., 2018; Petrosino et al., 2019).

The atomic partial charges were calculated in the frame of the Density Functional Theory (DFT) using two quantum approaches (De Luca et al., 2014): the Electro Static Potential (ESP) and the Löwdin methods as implemented in NWChem (Valiev et al., 2010) code. It is worthwhile remarking that the atomic partial charges were evaluated taking into account both the protonation and the de protonation of external amino acids according to the pH value related to the structure of the considered BSA, as shown in (De Luca et al., 2014). The ESP method allowed evaluating the atomic charges from the fitting of the quantum mechanical electro static potential on selected grid points centered on each of the atoms of the aforementioned calculated external surface (Curcio et al., 2018; Petrosino et al., 2019). Finally, the BSA total charge number, Z, was evaluated (De Luca et al., 2014). The computed total charge was in good agreement with the reported values (de la Casa et al., 2008; Fukuzaki et al., 1996). Moreover, it is important to emphasize that this fundamental property was calculated with out resorting to any adjustable parameter.

2.2. Colloid interaction potential energy

The study of colloidal interactions by MC simulations is very effective since it is explicitly based on the knowledge of the inter action potential, which depends on both the polydispersity and the volume fraction (Iacovella et al., 2010).

Here BSA is coarse grained as a sphere with a bare charge Z e given by QM calculations and an equivalent radius of a = 3.2 nm permitting to conserve the protein volume approximately. It is worthwhile noting that this value as also been exploited in the lit erature (Bowen and Williams, 1996). Though BSA exhibits a non zero dipole moment (Scheider et al., 1976), for the values of vol ume fractions considered in the present paper, the system showed a dominance of long range interactions where the dipole effect became negligible; hence, a coarse grained sphere was considered detailed enough to properly describe the behavior of BSA at long range.

The total potential energy was split up into three contributions. A hard sphere part, an electrostatic potential and a van der Waals potential. The hard sphere contribution was classically imple mented as:

$$\boldsymbol{U_{HS}(r_{ij})} \quad \begin{cases} \infty, \boldsymbol{r_{ij}} \le \sigma \\ 0, \boldsymbol{r_{ij}} > \sigma \end{cases} \tag{1}$$

where r_{ij} is the center to center distance and σ $2a$ the overlap limit distance between two interacting spheres.

The electrostatic repulsion potential can be considered as the characterizing part of the total interactions and is usually repre sented as the Static Screened Coulomb Potential (SSCP) also known as Yukawa Potential (YP). (Edwards et al., 2017) For two microion dressed charged colloid spheres of radius a at centre to centre dis tance r_{ij}, the YP can be modeled as:

$$\boldsymbol{U_{elc}(r_{ij})} \quad \boldsymbol{l_B Z_{eff}}^2 \left(\frac{\exp(\boldsymbol{k_{eff} a})}{1+\boldsymbol{k_{eff} a}}\right)^2 \frac{\exp(-\boldsymbol{k_{eff} r_{ij}})}{\boldsymbol{r_{ij}}} \boldsymbol{K_B T} \tag{2}$$

Which is valid for non overlapping spheres. Here, l_B $e^2/(4\pi\varepsilon_0\varepsilon_R K_B T)$ is the Bjerrum length of the suspending fluid and e, ε_0, ε_R, K_B and T, are, respectively, the electron charge, the void and relative dielectric constants, the Boltzmann constant and the operating temperature. Z_{eff} and k_{eff} are the colloid effective charge number and effective screening parameter, respectively. These parameters are equal to the bare charge Z and to the inverse Debye length k for dilute suspensions of weakly charged objects. In highly charged or concentrated suspensions, they can be computed from Z, k and the volume fraction with so called renormalization methods.

Even if the long range repulsive Yukawa potential is the charac terizing contribution in the considered system, the attractive con tributions should also be evaluated by the van der Waals (vdW) formulation: (Nägele, 2004)

$$\boldsymbol{U_{vdw}(r_{ij})} \quad \frac{\boldsymbol{A_{eff}}}{6}\left[\frac{2\boldsymbol{a}^2}{\boldsymbol{r_{ij}}^2 - 4\boldsymbol{a}^2} + \frac{2\boldsymbol{a}^2}{\boldsymbol{r_{ij}}^2} + \ln\left(1 - \frac{4\boldsymbol{a}^2}{\boldsymbol{r_{ij}}^2}\right)\right] \tag{3}$$

The effective Hamaker constant, A_{eff}, incorporates, to some extent, the electrodynamic retardation and non additivity effects on the dispersion forces. (Nägele, 2004)

For dispersions of highly charged colloidal particles, U_{vdw} becomes completely masked by the electrostatic part U_{elc}. In this case, the colloidal particles (with associated microion layer) are usually referred as Yukawa spheres, since their microstructural properties are determined only by the Yukawa like exponentially screened Coulomb potential U_{elc}. (Nägele, 2004) It is worthwhile remarking that, instead, for weakly charged colloidal particles, U_{vdw} was not masked and proteins would aggregate, under the combined effect of the van der Waals interactions at moderate dis tance and anisotropic, local, electrostatic interactions, close to con tact. The prediction of the cake close packed structure would thus require the extension of the present method to short range aniso tropic interactions. However, the computation of such complex interactions was far beyond the scopes of the present paper.

It is assumed that the total potential energy of a N particle liq uid system can be approximated by a sum of pair interactions. Under the premise of this pairwise additivity assumption, the ther modynamic and microstructural properties of the fluid are solely expressible in terms of $u_{tot}(r_{ij})$ $U_{HS}(r_{ij}) + U_{elc}(r_{ij}) + U_{vdw}(r_{ij})$ and of its associated Radial Distribution Function (RDF), $g(r)$ (Vlugt, 2009). It should be noted that the vdW term is sometimes negligi ble in the calculation of the osmotic pressure. It will be the case in the present work, as shown later.

2.3. Monte Carlo simulation method

The Monte Carlo (MC) method is a stochastic simulation proce dure especially suitable to problems involving particle(s) dynamics due to its capability to evaluate each discrete particle displace ment. (Chen et al., 2005) The used scheme for the implementation of the present simulation code is based on the Metropolis Monte Carlo approach thanks to which the total energy of the system, based on the exploited energy calculation, is used as a criterion for evaluating the acceptance or rejection of each single MC step.

The Metropolis method starts with a tentative random location of the considered system of particles. Defining an ensemble where the number of particles, simulation box volume and temperature are fixed (NVT ensemble), a set of particles coordinate can be ran domly evaluated inside the specified box (see Fig. 1).

The method proceeds with the random choice of a particle, its random displacement of a fixed distance δr_{max} and the evaluation of the MC move. One point to note is that it is necessary to protect against a trial move, which might result in a significant molecular overlap. However, with the implementation of the explained hard

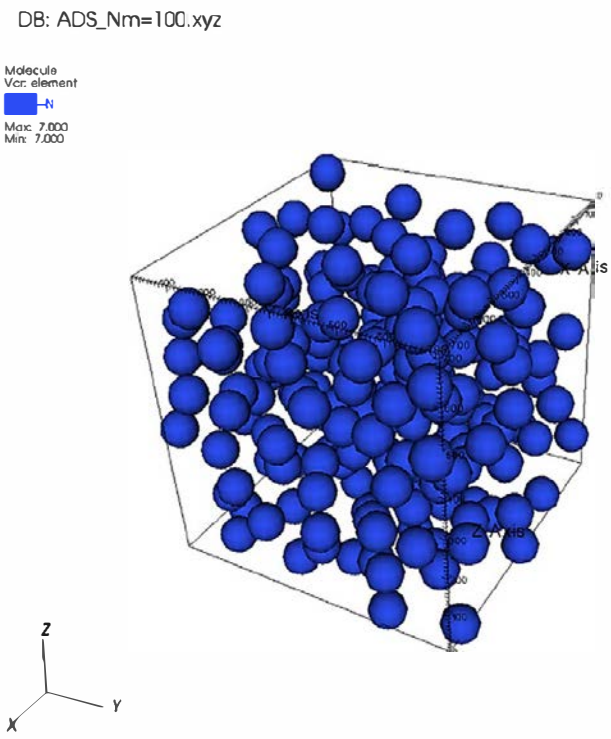

Fig. 1. First random configuration of an MC box. Box length = 65 nm.

sphere contribution in potential energy calculation, the colloids overlapping can be excluded.

The maximum allowed displacement δr_{max} governs the size of the trial MC move. If this parameter is too small, a large fraction of displacement is accepted but the phase space of the system is explored slowly. If δr_{max} is too large, nearly all the trial moves are rejected and the possible movement through the phase space is rather limited. An optimal value of δr_{max}, equal to colloid radius a, was therefore chosen to perform the simulations.

Several details on the implemented procedure will be presented hereafter in the subsequent sections of the manuscript.

2.4. Theoretical approaches

The structures resulting from the MC simulations were firstly compared to those calculated by solving the Omstein Zernike (OZ) equation with the Hypernetted Chain (HNC) closure (Howard and Frank, 1976).

The osmotic pressure calculation was performed by (Roa et al., 2016):

$$\frac{\beta\Pi}{n} \quad 1+4\pi\phi g(\sigma^{+}) \quad \frac{2\pi}{3}n\int_{\sigma}^{\infty}\frac{\partial\beta(U_{elc}+U_{vdw})(r)}{\partial r}g(r)r^{3}dr \qquad (4)$$

where β $1/(K_BT)$, n N_c/V was the colloidal number concentration, $g(\sigma^{+})$ was the RDF function value at r σ^{+}. The 1 on the right hand side is the ideal contribution. The second and third terms are contributions from contacts and non contact interactions, respectively. When using an effective potential such as U_{elc}, two other terms can appear in this relation. One is the so called "volume term" and the other is an integral involving a density derivative of U_{elc} (Boon et al., 2015). They are important when the effective charge and screening length differ significantly from their bare values. In the present work, the colloidal charge is quite low and the salt content quite high so renormalization has only a mild effect and these two terms can be omitted.

The concentration dependent collective diffusion coefficient, $D_c(\phi)$, was expressed as: (Roa et al., 2016)

$$D_c(\phi) \quad D_0\frac{K(\phi)}{\chi_{osm}} \qquad (5)$$

where D_0 $K_BT/(6\pi\eta_0 a)$ was the single particle diffusion coefficient, η_0 the water viscosity, $K(\phi)$ was the long time sedimentation coefficient (Roa et al., 2015) and χ_{osm} was the osmotic compressibility coefficient, which can be expressed as:

$$\frac{1}{\chi_{osm}} \quad \left.\frac{\partial(\beta\Pi)}{\partial n}\right|_T \qquad (6)$$

The reported long time sedimentation coefficient strongly depends on system interactions, which determine a significant change of settling particles structure; therefore, two limiting cases, referred respectively for Hard Sphere model (Richardson, 1954) (low interaction system) and Happel crystal model (Happel, 1958) (high interaction system) were taken into account and exploited in section 4 of the present paper.

A final expression for diffusion coefficient was therefore obtained as:

$$D_c(\phi) \quad \frac{2a^2}{9\eta_0}K(\phi)\left.\frac{\partial\Pi}{\partial\phi}\right|_T \qquad (7)$$

Starting from the total energy derived from the Monte Carlo simulations, Eqs. 4 7 allowed calculating both the Osmotic Pressure and the Diffusion Coefficient of BSA as a function of the volume fraction (or concentration) of colloids.

3. Numerical implementation

The complete multi scale framework implementation started from the ab initio knowledge acquired at both sub nanoscopic and nanoscopic scales, and was therefore independent on experimental or empirical information. The fundamental linking parameter, namely the BSA surface charge distribution, was exploited so to achieve the proper scale transition, allowing the calculation of the total, bare charge number, Z.

The MC simulations used to compute the osmotic pressure and the diffusion coefficient are based on the effective electrostatic potential U_{elc} involving an effective charge and an effective screening length. These parameters were obtained with the Extrapolated Point Charge (EPC) renormalization method (Boon et al., 2015) with the bare charge Z computed with Quantum Mechanics as input parameter.

The other required inputs of MC simulations were: the number of adsorbed molecules, N, the simulation box volume fraction, ϕ, the system temperature, T, the Boltzmann Constant K_B, the minimum distance, σ, the radius, a, the maximum number of iterations, *max_iter*, the overlapping energy limit U_{tot_max}, which represents the highest energy value of overlapped spheres in the hard sphere energy approach, the parameter *d_gr*, which represented the number of MC steps whenever the box structure and the RDF files are saved, the parameter *lay_tick* used to define the layer thickness in the calculation of the RDF and the *seed* value used to control the random generation (Matsumoto and Nishimura, 1998).

A total potential energy code was implemented in agreement with Eqs. (1) (3) for a macromolecules coordinates matrix. The $\varepsilon_0, \varepsilon_R$ and A_{eff} constants were defined within the simulation code.

For each volume fraction, ϕ, 8 sets of simulations were performed with 8 different seeds related to the number of available processors. For each of the considered seeds, a *max_iter* number of MC iterations were performed.

A characteristic number of MC iterations n_{MCch} was set on the basis of the steps, which were actually necessary to notice an initial

decrease in system energy. After different tests, a number of $3n_{MCch}$ accepted displacements was considered as adequate to obtain satisfactory RDFs and osmotic pressure results.

Two Intel Xeon CPU E5 2609 v2 processors were used on 8 cores and the calculation times in the case of high volume fractions were equal, on average, to about 72 h.

4. Results and discussions

In this section, the fundamental results deriving from sub nano and nanoscopic scales are firstly illustrated, together with the results of MC simulations calculated in a range of concentrations deriving from the flux decay profiles characterizing the ultrafiltration process (De Luca et al., 2014; Curcio et al., 2018). The validation of MC code carried out by the Hypernetted Chain (HNC) theory (Hallez and Meireles, 2017) is then presented. Finally, the calculations of the Osmotic Pressure and the Diffusion Coefficient for an experimental study available in the literature (Bowen and Williams, 1996), are reported. The theoretical calculations of the Osmotic Pressure were performed by the HNC theory too. It was then possible to carry out both a theoretical analysis and an experimental validation of the formulated computational model.

4.1. Ab initio total protein charge and minimum distance

The surface charges distribution calculation was performed by the ESP method (De Luca et al., 2014; Curcio et al., 2018; Zeng et al., 2013). At pH = 7, the external amino acids functional groups were protonated or deprotonated as described in section 2.1. The surface charges were used to evaluate the protein total charge, obtaining 15.82 atomic units. Consequently, the colloid charge number Z = 15.82 was used as a bare charge in the model.

The exploited radius was equal to a 32Å (Bowen and Williams, 1996). The center to center minimum distance among the adsorbed proteins, σ 64Å, was imposed as the lower bound in total energy calculation for MC simulation.

4.2. MC simulation sets and code validation

An NVT ensemble was defined to perform the MC simulations. A set of volume fractions was defined in agreement with a previously obtained ultrafiltration concentration polarization profiles (Curcio et al., 2018) as illustrated in Fig. 2. Referring to Fig. 9 of previous work (Curcio et al., 2018) the disperse cake profile was analyzed. The deriving concentration diagram for an ultrafiltration time of 3200s, a transmembrane pressure of 1.5bar and a membrane rejection of 0.9875, was discretized. Different characteristic points as a set of corresponding volume fractions were obtained.

Thanks to these considerations, a volume fraction, ϕ, ranging between 0.05 and 0.30 was chosen. As a trade off between a high enough box dimension and an affordable computer effort, a number of BSA colloids, N, equal to 200 was chosen. From a fixed N and ϕ the simulation box volume was calculated and the resulting box length ranged from 45 to 82 nm. The other input parameters were T 300K, max_$iter$ 1.5 10^4, U_{tot_max} $10^{13}J$, d_gr 100, lay_tick 2Å. The ε_R constant was fixed equal to the water dielectric constant, ε_R 81.07 and A_{eff} 1.354 $10^{-20}J$.

For MC calculations validation a total charge number Z 15.82 was set up. A ionic strength, I 0.15M, was analyzed in order to compare the simulation results as provided by the present multi scale model to the experimental data reported in the literature (Bowen and Williams, 1996), giving a screening parameter equal to k $1/(8.0068\ 10^{-10})$ $1.25\ 10^9$. However, the renormalization procedure (Boon et al., 2015) was performed, and yielded Z_{eff} 15.56 and k_{eff} $1.27\,10^9$. Both the values are practically coincident with the ones corresponding to the non renormalized parameters (Z 15.82, k $1.25\ 10^9$) for the considered conditions.

As shown in Fig. 3, after 5000 MC iterations the total energy was stable with a rather small fluctuation around the equilibrium state.

The Metropolis algorithm was first validated in the case of hard sphere interactions (Fig. 4).

Then, for a more complete test, the RDFs produced by MC simulations considering both hard sphere collisions and effective electrostatic interactions were also compared to RDFs calculated

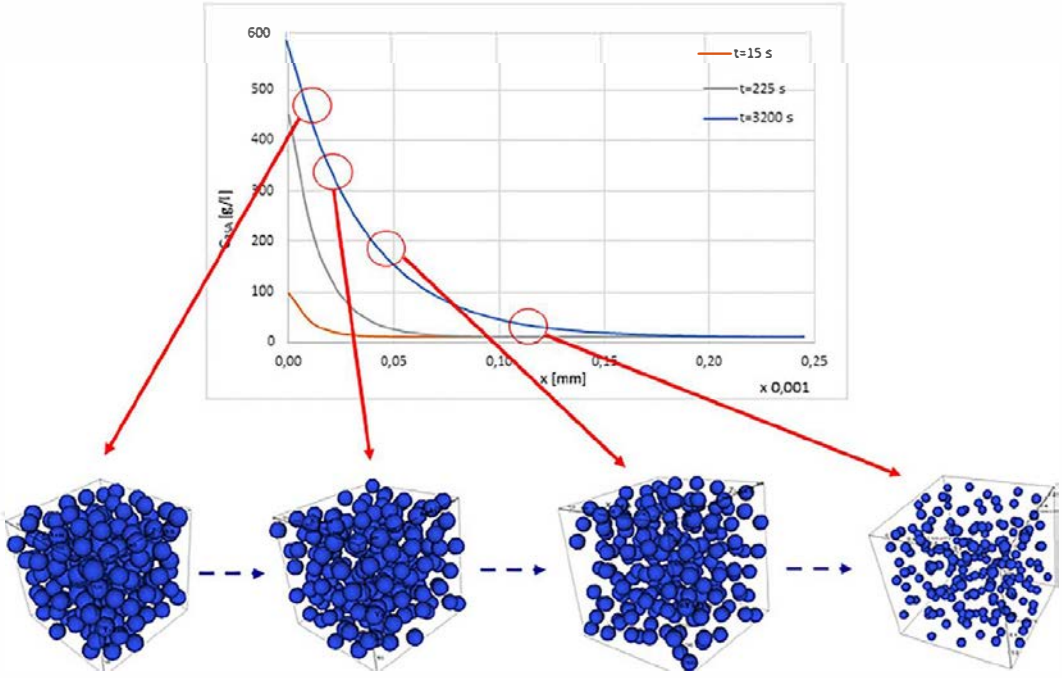

Fig. 2. Concentration-polarization profile discretization for a volume fraction set choice. BSA ultrafiltration on polysulfone membrane TMP = 1.5 bar, membrane Rejection Rej = 0.9875, for a filtration time of 3200 s (considered curve) (Curcio et al., 2018).

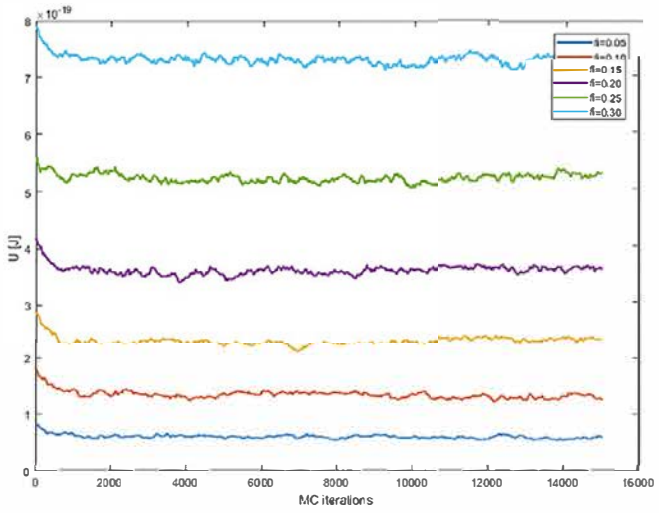

Fig. 3. Total energy profile as function of MC iterations for different volume fractions. Z 15.82, I 0.15M, pH 7, a 32Å, σ 64Å, T 300K

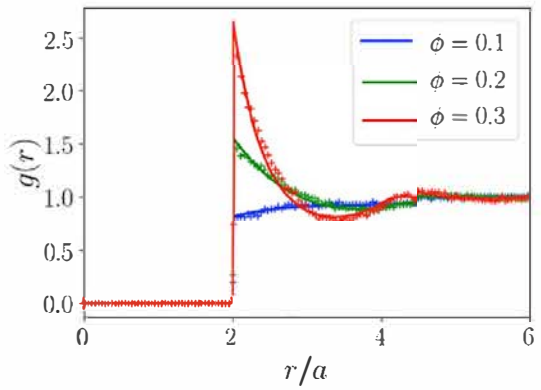

Fig. 4. Hard-Sphere potential RDFs validations. + is the MC simulation points, lines the HNC theory results. r/a is the normalized distance with colloids radius a. Z 15.82, I 0.15M, pH 7, a 32Å, σ 64Å, T 300K

theoretically with HNC. As shown in Figs. 4 and 5 a very good agreement between these techniques can be observed for hard sphere and Yukawa type electrostatic potential, which validates our MC implementation.

The Yukawa case shows $g(2a) \rightarrow 0$, which means that contacts are not much present.

Therefore, it was decided to perform some other simulations without considering the van der Waals contribution.

4.3. Osmotic pressure and diffusion coefficient

Once the MC model was validated, different sets of simulations were performed on the basis of the previously defined total bare charge number Z and screening parameter k.

The energy set from MC simulations is reported in Fig. 6.

The total Yukawa energy compared to the K_BT value is $0.5K_BT$ energy per colloid particle.

The osmotic pressure was carried out using Eq. (4). Moreover, in order to achieve the experimental validation of the present model, a set of data reported in *Bowen et al.* paper (Bowen and Williams, 1996), were taken as reference. A comparison of MC results with both HNC theory and *Bowen et al.* data (Bowen and Williams, 1996) is reported in Fig. 7.

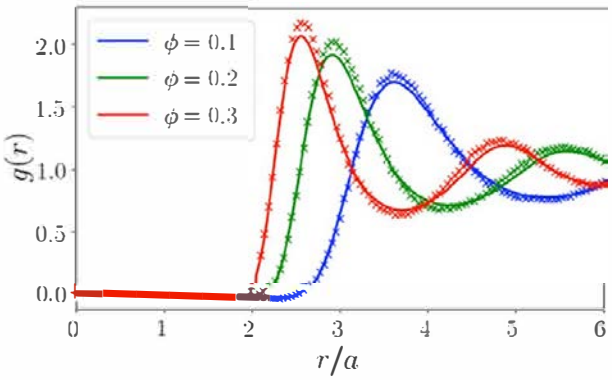

Fig. 5. Yukawa potential RDFs validations. + is the MC simulation points, lines the HNC theory results. r/a is the normalized distance with colloids radius a. Z 15.82, I 0.15M, pH 7, a 32Å, σ 64Å, T 300K

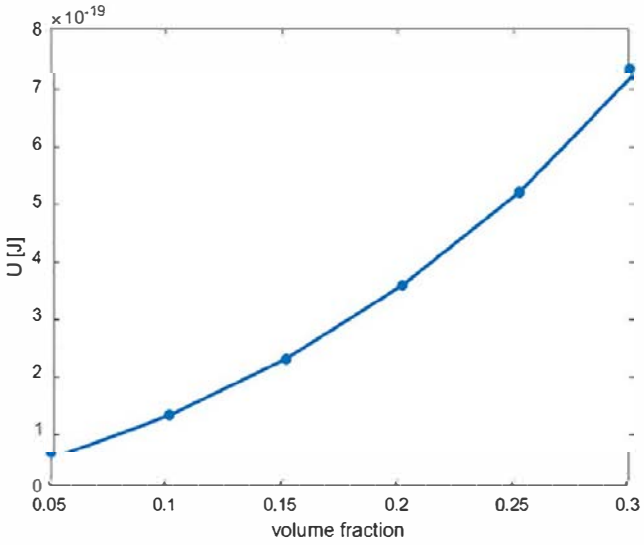

Fig. 6. Total energy as function of volume fraction for Yukawa potential total energy. Z 15.82, I 0.15M, pH 7, a 32Å, σ 64Å, T 300K

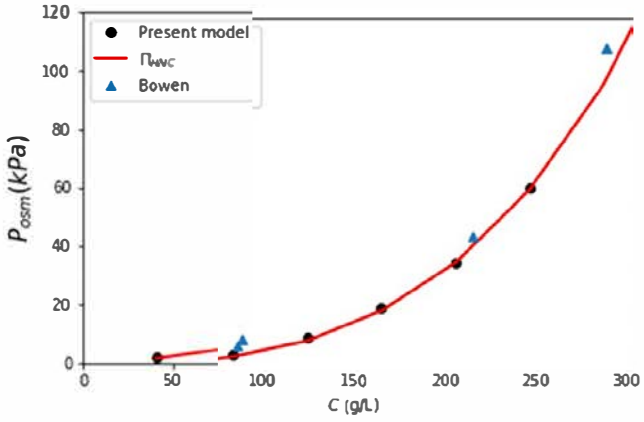

Fig. 7. Osmotic pressure comparison as function as colloid concentration between the presented model Monte Carlo results (black dots), HNC theory results (red line) and experimental data. Ionic Strength 0.15 M, pH = 7. Concentration in g/L in agreement with literature (Bowen and Williams, 1996).

The results show a good agreement between the present multi scale theoretical model, based both on the ab initio knowledge acquired at sub nanoscopic scale and on MC simulations, and the experimental data, with maximum relative errors equal to 6%.

Once the pressure calculation has been validated, basing on the Eq. (4), three osmotic pressure contributions were analyzed and reported in Fig. 8.

The linear colloidal ideal gas contribution P_{id} denoted a medium of 15% of the total pressure. However, for very dilute system it rep resented the characterizing contribution due to the assimilation of the system to an ideal one. The contact and non contact interaction pressure contributions contributed more or less equally to the total pressure. As expected, at high concentrations these interaction contributions dominate the total pressure.

At this level it is possible to derive an important transport prop erty of the deposit layer starting from sub nanoscopic information, the diffusion coefficient (using Eqs. (5) (7)) if the sedimentation coefficient $K(\phi)$ is known. $K(\phi)$ is a hydrodynamic function depend ing on the suspension structure, and is thus still unknown for arbi

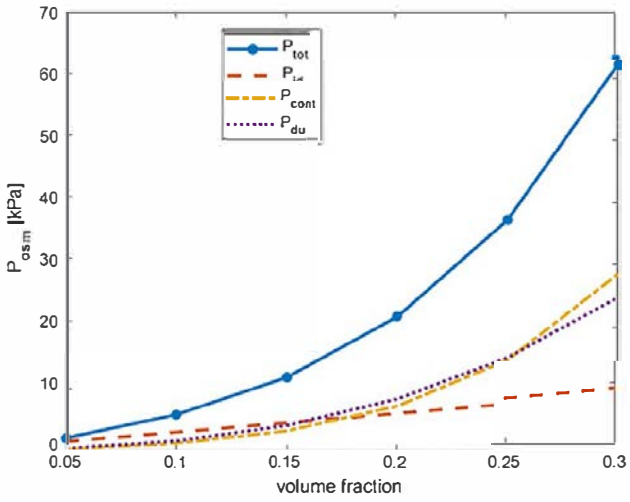

Fig. 8. Model predicted osmotic Pressure of the fouling cake as function of volume fraction during ultrafiltration process for Yukawa potential formulation. Total osmotic pressure in continuous line and the three different contributions basing on Eq.4. Z 15.82, I 0.15M, pH 7, a 32Å, σ 64Å, T 300K. Process conditions: TMP = 1.5 bar, Rej = 0.9875, t = 3200 s.

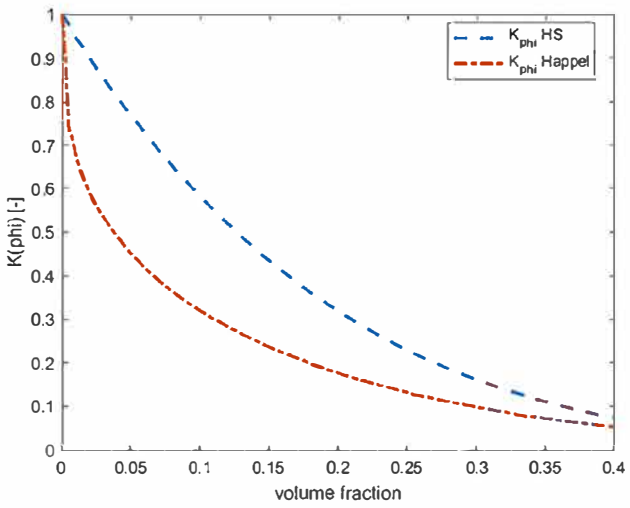

Fig. 9. Sedimentation coefficient, $K(\phi)$, comparison between Hard Sphere model and Happel model calculations.

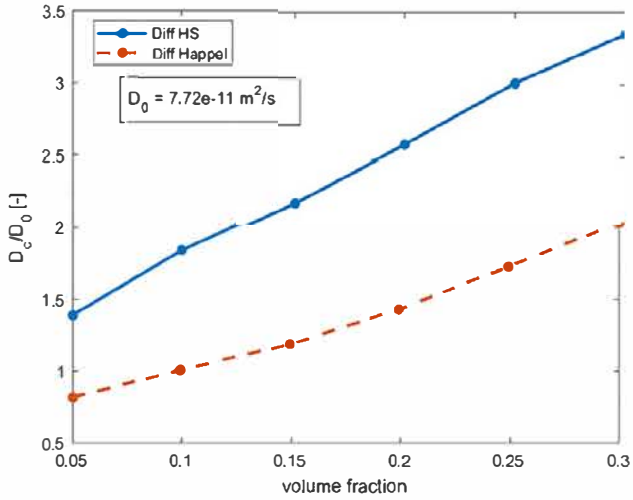

Fig. 10. Model predicted diffusion coefficient, D_c/D_0, of the fouling cake as function of volume fraction during ultrafiltration process for Yukawa potential formulation. Both hard sphere and Happel models were implemented for $K(\phi)$ calculation. D_0 $7.72 \cdot 10^{-11}\ \frac{m^2}{s}$, Z 15.82, I 0.15M, pH 7, a 32Å, σ 64Å, T 300K. Process conditions: TMP 1.5bar, Rej 0.9875, t 3200s.

trary colloidal interactions. In what follows, we therefore report two diffusion coefficient calculations based on the two extreme pictures of vanishing electrostatic interactions (the Hard Sphere model) and strongly repulsive interactions (a solide like suspension).

For the Hard Sphere case, the Richarson and Zaki correlation (Richardson, 1954) was implemented as $K(\phi)$ $(1 \quad \phi)^{\alpha}$ with the now well accepted exponent α 5.1 (see Ref. (Lecampion and Garagash, 2014) for nice comparison of $K(\phi)$ for hard spheres). Instead, for strongly repulsive systems colloids remain far from each other during sedimentation and the solution of Happel's cell model (Happel, 1958) is better suited. It reads $K(\phi)$ $\frac{3}{2}\frac{\frac{9}{2}\gamma+\frac{9}{2}\gamma^5}{3+2\gamma^5}\frac{3\gamma^6}{}$ with γ $\sqrt[3]{\phi}$. These two sedimentation coefficient models are reported in Fig. 9 and the corresponding diffusion coefficients are reported in Fig. 10.

The diffusion coefficient trend presented a smooth rising trend in agreement with similar literature data (Roa et al., 2016). This is the signature of repulsive electrostatic interactions promoting the classical Brownian collective diffusion.

In the case of the Happel model, lower values of diffusion coef ficient were observed, since particle repulsion is strong, thus deter mining a particle arrangement represented by a crystal or glass; in this case friction is important since the fluid flow has to occur through a high number of tiny spaces. Instead, in the case of the Hard Sphere model, particle tend to form at least some couples which results in wider spaces available for the fluid and, therefore, in lower friction and a higher diffusion coefficient.

5. Conclusions

In the present work, key macroscopic quantities of ultrafiltra tion processes, i.e. osmotic pressure and diffusion coefficient, were obtained starting from the BSA surface charges through a rigorous quantum ab initio method regardless of any empirical parameters at fixed pH. The very crucial quantity, the colloid charge number, was exploited from quantum mechanics approach rather than using different experimental fitted values. It is worthwhile empha sizing that the present work makes use of different theories and merges all of them according to a real multiscale approach which starts at sub nanoscopic scale.

In other previous works a fouling modelling approach in UF pro cesses considered equilibrium quantities to characterize the adsorbed compact cake and classical force balance for the descrip tion of loose layers. In the present one a stochastic approach, based on a metropolis MC method, was used to describe the fouling for mation. The formulated model was validated by well assessed col loid physics theoretical methods and a very good agreement was actually observed.

Moreover, a good agreement between osmotic pressure and corresponding experimental data taken from the literature was remarked.

Quantum Mechanics is a powerful tool to access detailed prop erties of colloids involved in UF, but its application is limited to the scale of one object and it does not account for entropic effects driv ing the meso structure of colloidal dispersions. On the other hand, Monte Carlo simulations are designed to capture the structuration at this meso scale, but they require the detailed characteristics of colloids (as the surface charge) as input parameter.

The multiscale framework presented here combines these two approaches to get the best of both worlds. It can be used as a "first brick" for different processes simulations, as a mean to com pute thermodynamic and transport properties of colloidal disper sions. In addition, this multiscale framework could be used to predict partial or total aggregation for example.

The next step would be to introduce a third component at even large scale: the transport coefficients, computed from the present multiscale framework, can be considered as input parameters for a continuous description of mass and momentum transfers at the scale of processes with a Computational Fluid Dynamics approach. This will be conducted using MC box meshes in CFD simulations obtaining different fouling cake properties, such as the cake permeability.

CRediT authorship contribution statement

F. Petrosino: Conceptualization, Software, Validation, Formal analysis, Investigation, Data curation, Writing original draft, Visu alization. **Y. Hallez:** Conceptualization, Methodology, Resources, Writing review & editing, Supervision. **G. De Luca:** Conceptualiza tion, Methodology, Validation, Writing review & editing, Supervi sion. **S. Curcio:** Conceptualization, Resources, Writing review & editing, Supervision, Project administration, Funding acquisition.

Declaration of Competing Interest

The authors declare that they have no known competing finan cial interests or personal relationships that could have appeared to influence the work reported in this paper.

Appendix

Nomenclature

a	Protein radius	[m]
A_{eff}	Effective Hamaker constant	[J]
d_gr	MC steps files saving	[ ]
D_c	Diffusion coefficient	$[m^2/s]$
D_0	Single particle diffusion coefficient	$[m^2/s]$
e	Electron charge ($1.60217646 \ 10^{-19}$)	[C]
$g(r)$	Radial distribution function	[ ]
k	Inverse of Debye length	$[m^{-1}]$
K	Long time sedimentation coefficient	[ ]
K_B	Boltzmann constant ($1.3806503 \ 10^{-23}$)	[J/K]
l_B	Bjerrum length	[m]
lay_tick	RDF layer thickness	[A]
max_iter	Maximum number of MC iterations	[ ]
n	Colloidal number concentration	$[m^{-3}]$
n_{MCch}	Characteristic MC steps number	[ ]
n_{res}	Reservoir ion density	$[m^{-3}]$
N_c	Number of colloids	[ ]
r_{ij}	Proteins centre to centre distance	[m]
$seed$	Seeds MC number	[ ]
T	Temperature	[K]
TMP	Transmembrane pressure	[Pa]
U_{elc}	Electrostatic energy contribution	[J]
U_{HS}	Hard Sphere energy contribution	[J]
U_{tot}	Total interaction energy (=A)	[J]
U_{vdw}	van der Waals energy contribution	[J]
U_{tot_max}	Overlapping energy limit	[J]
V	Simulation volume	$[m^3]$
V_c	Total volume of colloids	$[m^3]$
Z	Colloid charge number	[ ]
β	Energy constant (=$1/(K_BT)$)	$[J^{-1}]$
δr_{max}	Random displacement	[m]
ε_R	Relative dielectric constant (81.07)	[ ]
ε_0	Void dielectric constant $8.8541878 \ 10^{-12}$	$[C^2/(Jm)]$
η_0	Water viscosity	[Pa s]
Π, P_{osm}	Osmotic pressure	[Pa]
σ	Centre to centre minimum distance	[m]
ϕ	Volume fraction	[ ]
$\boldsymbol{\chi_{osm}}$	Osmotic compressibility coefficient	[ ]

References

Barbosa, L.R.S., Ortore, M.G., Spinozzi, F., Mariani, P., Bernstorff, S., Itri, R., 2010. The importance of protein-protein interactions on the PH-induced conformational changes of bovine serum albumin: a small-angle X-ray scattering study. Biophys. J.

Bolton, G., LaCasse, D., Kuriyel, R., 2006. Combined models of membrane fouling: development and application to microfiltration and ultrafiltration of biological fluids. J. Memb. Sci. 277, 75–84.

Boon, N., Guerrero-García, G.I., Van Roij, R., De La Cruz, M.O., 2015. Effective charges and virial pressure of concentrated macroion solutions. Proc. Natl. Acad. Sci. U. S. A. 112, 9242–9246.

Bowen, W.R., Williams, P.M., 1996. The osmotic pressure of electrostatically stabilized colloidal dispersions. J. Colloid Interface Sci. 184, 241–250.

Braga, C., Smith, E.R., Nold, A., Sibley, D.N., Kalliadasis, S., 2018. The pressure tensor across a liquid-vapour interface. J. Chem. Phys. 149, 044705.

Chakraborty, S., Loutatidou, S., Palmisano, G., Kujawa, J., Mavukkandy, M.O., Al-Gharabli, S., Curcio, E., Arafat, H.A., 2017. Photocatalytic hollow fiber membranes for the degradation of pharmaceutical compounds in wastewater. J. Environ. Chem. Eng. 5, 5014–5024.

Chen, J.C., Elimelech, M., Kim, A.S., 2005. Monte Carlo simulation of colloidal membrane filtration: model development with application to characterization of colloid phase transition. J. Memb. Sci. 255, 291–305.

Chen, Y., Kim, H., 2008. Monte Carlo simulation of pore blocking and cake formation by interfacial interactions during membrane filtration. Desalination 233, 258–266.

Cheng, T.W., Yeh, H.M., Gau, C.T., 1998. Flux analysis by modified osmotic-pressure model for laminar ultrafiltration of macromolecular solutions. Sep. Purif. Technol. 13, 1–8.

Curcio, S., Petrosino, F., Morrone, M., De Luca, G., 2018. Interactions between proteins and the membrane surface in multiscale modeling of organic fouling. J. Chem. Inf. Model. 58 (9), 1815–1827.

de la Casa, E.J., Guadix, A., Ibáñez, R., Camacho, F., Guadix, E.M., 2008. A combined fouling model to describe the influence of the electrostatic environment on the cross-flow microfiltration of BSA. J. Memb. Sci. 318 (1–2), 247–254.

De Luca, G., Bisignano, F., Paone, F., Curcio, S., 2014. Multi-scale modeling of protein fouling in ultrafiltration process. J. Memb. Sci. 452, 400–414.

Deserno, M., von Grünberg, H.H., 2002. Osmotic pressure of charged colloidal suspensions: a unified approach to linearized poisson-boltzmann theory. Phys. Rev. E. Stat. Nonlin. Soft Matter Phys. 66, 011401.

Edwards, J.P., Gerber, U., Schubert, C., Trejo, M.A., Weber, A., 2017. The Yukawa potential: ground state energy and critical screening. Prog. Theor. Exp. Phys. 2017, 083A01.
Flora, J.R.V., 1993. Stochastic approach to modeling surface fouling of ultrafiltration membranes. J. Memb. Sci. 76, 85–88.
Fukuzaki, S., Urano, H., Nagata, K., 1996. Adsorption of bovine serum albumin onto metal oxide surfaces. J. Ferment. Bioeng. 81 (2), 163–167.
Hallez, Y., Meireles, M., 2017. Fast, robust evaluation of the equation of state of suspensions of charge-stabilized colloidal spheres. Langmuir 33, 10051–10060.
Hansen, J.P., McDonald, I.R., Theory of Simple Liquids, 4th ed.; Press, A., Ed.; Academic Press, 2006.
Happel, J., 1958. Viscous Flow in multiparticle systems: slow motion of fluids relative to beds of spherical particles. AIChE J. 4 (2), 197–201.
Howard, L., Lemberg; Frank H. Stillinger, 1976. Application of Hypernetted-Chain Integral Equations to a Central-Force Model of Water, 32 (2), 353–362.
Iacovella, C.R., Rogers, R.E., Glotzer, S.C., Solomon, M.J., 2010. Pair interaction potentials of colloids by extrapolation of confocal microscopy measurements of collective suspension structure. J. Chem. Phys. 133, 164903.
Lecampion, B., Garagash, D.I., 2014. Confined flow of suspensions modelled by a frictional rheology. J. Fluid Mech.
Matsumoto, M., Nishimura, T., 1998. Mersenne Twister: a 623-dimensionally equidistributed uniform pseudo-random number generator. ACM Trans. Model. Comput. Simul. 8, 3–30.
Nägele, G., 2004. The physics of colloidal soft matter. Mater. Struct. 2, 674–688.
Nath, A., Mondal, S., Chakraborty, S., Bhattacharjee, C., Chowdhury, R., 2014. Production, purification, characterization, immobilization, and application of β-galactosidase: a review. Asia-Pacific J. Chem. Eng. 9, 330–348.
F Richardson, J.; N. Zaki, W., 1954. Sedimentation and Fluidization: Part I. Trans. Inst. Chem. Eng.
Roa, R., Zholkovskiy, E.K., Nägele, G., 2015. Ultrafiltration modeling of non-ionic microgels. Soft Matter.
Roa, R., Zholkovskiy, E.K., Nägele, G., 2015. Ultrafiltration modeling of non-ionic microgels. Soft Matter 11, 4106–4122.
Petrosino, F., Curcio, S., Chakraborty, S., De Luca, G., 2019. Enzyme Immobilization on Polymer Membranes: A Quantum and Molecular Mechanics Study. Computation MDPI 7 (4), 56. https://doi.org/10.3390/computation7040056.
Roa, R., Menne, D., Riest, J., Buzatu, P., Zholkovskiy, E.K., Dhont, J.K.G., Wessling, M., Nägele, G., 2016. Ultrafiltration of charge-stabilized dispersions at low salinity. Soft Matter 12, 4638–4653.
Saha, K., R, U. M., Sikder, J., Chakraborty, S., da Silva, S. S., dos Santos, J. C., 2017. Membranes as a tool to support biorefineries: applications in enzymatic hydrolysis, fermentation and dehydration for bioethanol production. Renew. Sustain. Energy Rev. 2017, 74, 873–890.
Scheider, W., Dintzis, H.M., Oncley, J.L., 1976. Changes in the electric dipole vector of human serum albumin due to complexing with fatty acids. Biophys. J.
Stell, G., Joslin, C.G., 1986. The Donnan equilibrium: a theoretical study of the effects of interionic forces. Biophys. J. 50, 855–859.
Suki, A., Fane, A.G., Fell, C.J.D., 1984. Flux decline in protein ultrafiltration. J. Memb. Sci. 21, 269–283.
Szymczyk, A., Fievet, P., 2005. Investigating transport properties of nanofiltration membranes by means of a steric, electric and dielectric exclusion model. J. Memb. Sci. 252 (1–2), 77–88.
Valiev, M., Bylaska, E.J., Govind, N., Kowalski, K., Straatsma, T.P., Van Dam, H.J.J., Wang, D., Nieplocha, J., Apra, E., Windus, T.L., et al., 2010. NWChem: A comprehensive and scalable open-source solution for large scale molecular simulations. Comput. Phys. Commun. 181 (9), 1477–1489.
Vlugt, T.J.H., 2009. Introduction to Molecular Simulation and Statistical Thermodynamics.
Zeng, J., Duan, L., Zhang, J.Z.H., Mei, Y., 2013. A numerically stable restrained electrostatic potential charge fitting method. J. Comput. Chem. 34, 847–853.
Zin, G., Penha, F.M., Rezzadori, K., Silva, F.L., Guizoni, K., Petrus, J.C.C., Oliveira, J.V., Di Luccio, M., 2016. Fouling control in ultrafiltration of bovine serum albumin and milk by the use of permanent magnetic field. J. Food Eng. 168, 154–159.